Exploratory Investigation of Emissions from Flares with Non-hydrocarbon Liquids in the Flare Stream

Mohsen Kazemimanesh[†], Larry W. Kostiuk[†], Matthew R. Johnson[‡], D Nobes[†], Jason S. Olfert[†*]

[†] *Department of Mechanical Engineering, University of Alberta*
Edmonton, AB, T6G 2G8, Canada

[‡] *Department of Mechanical & Aerospace Engineering, Carleton University*
Ottawa, ON, K1S 5B6, Canada

Abstract

This research is an exploratory investigation into the effects of non-hydrocarbon liquids on flare gas phase and particulate emissions. The flaring process was simulated using a 9.45 mm diameter, natural gas diffusion flame with a 65 mm diameter co-flow air where liquids are introduced into the fuel stream using an ultrasonic atomizer. Various liquids were tested including distilled water and water with sodium chloride (to represent the naturally occurring saline water found at upstream oil and gas sites). Two flow rates of natural gas were considered: 0.3 standard liters per minute (mean velocity of 0.07 m/s) and 0.8 standard liters per minute (mean velocity of 0.2 m/s). The higher flow rate case was above the smoke point for the flame and produced soot particles in the exhaust. . An ultrasonic nozzle was used at the base of the stack to inject liquid droplets into the fuel stream. The focus of this exploratory research was to measure the size and number concentration of the emitted particulate matter (PM). Particle size distributions were obtained using a Scanning Mobility Particle Sizer (SMPS) for each flow condition, with and without liquid droplets injected into the fuel stream. The results showed that particulate matter emissions were orders of magnitude higher when salt water was present during the combustion of natural gas. Gas phase emissions were measured for the case of sooting diffusion flame using a portable gas analyzer. Results showed a decrease in soot and NOx emissions when distilled water was present in the fuel stream. Results also revealed that NOx emissions decreased and particulate emissions significantly increased when salt water was added to the flow, however, the additional particles did not appear to be soot. In addition, a sharp increase in hydrocarbon emissions was observed when salt water was combusted in the flame due to incomplete combustion. Moreover, investigation of volatility of particulate emissions when non-distilled water was present in the fuel stream showed that these particulate emissions are non-volatile.

1. Introduction

It is a common practice in the oil, gas and petrochemical industries to dispose of undesired flammable gases by either flaring or venting. Venting is simply the release of undesired gases to the atmosphere, while flaring is the combustion of gases in an open-atmosphere flame. Flaring is preferred to simply venting the gases since the mass-based global warming potential of CO_2 is approximately 25 times lower than that of methane on a 100-year time horizon [1]. The United States Energy Information Administration estimated that 122 billion m^3 of gas was flared or vented worldwide in 2008 [2], of which Alberta was responsible for approximately 1.14 billion m^3 [3].

Fracturing fluids have been utilised successfully for many years in the oil and gas industry for the purpose of increasing the extraction rates and recovery of oil and gas from well-sites. This process is based on the injection of highly-pressurized fracturing fluid into the wellbore to induce fractures and cracks in rock layers, which increases permeability and enables access to oil and gas reservoirs that would be otherwise isolated from the well. Fracturing fluids usually contain a proppant to keep the induced hydraulic fracture open, after removal of the pressurized fracturing fluids. Fracturing fluids and proppants currently used in industry vary considerably in composition based on geological data of the well site, and their exact composition and formulation remain proprietary in most cases. Some studies show that the major components of fracturing fluid are water, sodium chloride (which allows a delayed breakdown of the gel-polymer chains), and acids (mostly hydrochloric acid, which helps dissolve minerals and initiate fissure in the rock), hydrocarbons, and polymers [4][5][6]. A recent study reveals that in the United

* Corresponding author: Tel: +1-780-492-2341; Fax: +1-780-492-2200; E-mail: jolfert@ualberta.ca
Address: 5-1C Mechanical Engineering Building, University of Alberta, Edmonton, Alberta, T6G 2G8, Canada

States, approximately 3 billion liters (780 million US gallons) of hydraulic fracturing products (i.e. salt solutions and acids) have been used in fracturing operations between 2005 and 2009 [7].

Based on the significant amount of fracturing fluid used by the oil and gas industry, the general public and government regulators have voiced concerns in recent years about the possible effects of these fluids on ground water and air quality. The motivation behind this study was to conduct exploratory experiments to evaluate potential effects of non-hydrocarbon liquids on gas flare emissions. A possible scenario at upstream battery sites is that these fracturing fluids can enter the flare gas stream as droplets during the separation process and can be burned in the flare. The majority of the liquid is likely brackish water but hydraulic fracturing products may also be present. This paper presents particle-phase emissions measurements from a small laboratory flame during the combustion of natural gas with water and salt-water droplets, which are the major components of fracturing fluid.

2. Experimental Setup

To investigate the effects of distilled water, tap water, and salt water on flare emissions, a co-flow diffusion flame burner (9.45-mm diameter fuel tube surrounded by a 65-mm diameter co-flow air stream) was used. An ultrasonic atomizer attached to the base of the burner was used to introduce liquid droplets into the natural gas fuel stream prior to combustion. There are many droplet generation systems available; however, this study required evaluating the effects of varying the liquid mass flow independently from the gas stream flow rate. For this reason, the droplet generation system could not use flare gas to produce liquid droplets (such as airblast atomizers). The major benefit of utilizing an ultrasonic atomizer was that the delivery flow rate of liquid was independent from natural gas flow rate.

The experimental setup is represented schematically in Figure 1. The burner consists of a chamber, with the atomizer fitted at its base, where the natural gas stream and liquid droplets mix. This mixed flow exits the top of the chamber through a half-inch NPT tube fitting on which the flame is anchored. Air for combustion is provided through a co-flowing arrangement. This air enters the base of the burner through four equally spaced inlet ports and subsequently passes through a flow straightener mounted around the fuel tube fitting. A 72-mm diameter quartz tube was fitted around the air straightener, which prevented entrainment of ambient air. The length of quartz tube was selected to match the variable diffusion flame heights encountered in the experiments. For the purpose of sampling the emissions, a stainless steel tubular probe was fitted near the top of the quartz tube. Mass flow controllers were used to control the natural gas and air flow rates. Two flow conditions were considered. For condition one, the natural gas mass flow rate and air mass flow rate were 0.3 slpm (standard litres per minute at 1 atm and 25°C) and 13.4 slpm. For condition two, the fuel and air flow rates were 0.8 slpm and 18.0 slpm respectively. The higher flow rate condition exceeded the smoke point of the flame and produced higher amounts of soot in the exhaust stream. To measure the net liquid flow rate entering the flame, i.e. the flow rate of liquid exiting the top of the stack, the mass of the liquid in the pressurized vessel feeding the atomizer and the mass of liquid in the drain flask were measured as a function of time using a digital scale. The pressurized liquid vessel and drain flask were both placed on the scale so that the change in scale reading was a direct measure of the net mass transferred within a specified time interval. Steady-state tests showed that by setting the input flow rate at 5.5 mL/min, approximately 0.1 mL/min (~1.8%) of the liquid droplets passed out of the stack and into the flame zone.

The ultrasonic atomizer used in this study was manufactured by Sono-Tek, and was equipped with a broadband ultrasonic generator. Operating at the frequency of 120 kHz, the atomizer nozzle can deliver droplets with number median diameter equal to 19 μm and a geometric standard deviation of 1.84. The liquid spray created by the atomizer had a conical shape and the burner was designed so that natural gas flowed upward from the gap around the atomizer nozzle to entrain a maximum number of liquid droplets. The optimum point for generation of liquid droplets was found by varying the power of the broadband ultrasonic generator, which was set at 4 kW. Below this point, broadband generator was not able to effectively atomize the liquid into droplets.

Particle size distribution measurements were made by scanning mobility particle sizer (SMPS) manufactured by TSI Inc. The SMPS used in this study consists of a differential mobility analyzer (DMA) model 3081 and condensation particle counter (CPC) model 3776. The DMA classifies particles by their electrical mobility, which is related to the particle size. In the DMA, an electric field is created, and the airborne particles drift in the DMA according to their electrical mobility. Particle size is then calculated from the mobility distribution. The CPC operating principle is based on enlarging small particles so that they become visible to the optical instruments. Particles are continuously

drawn into the instrument and passed through a warm butanol vapor. The mixture then flows through a condenser section where the butanol vapor condenses onto the particles and "grows" them into larger droplets. The individual droplets then pass through the focal point of a laser beam, producing a pulse of light detected by a photodetector.
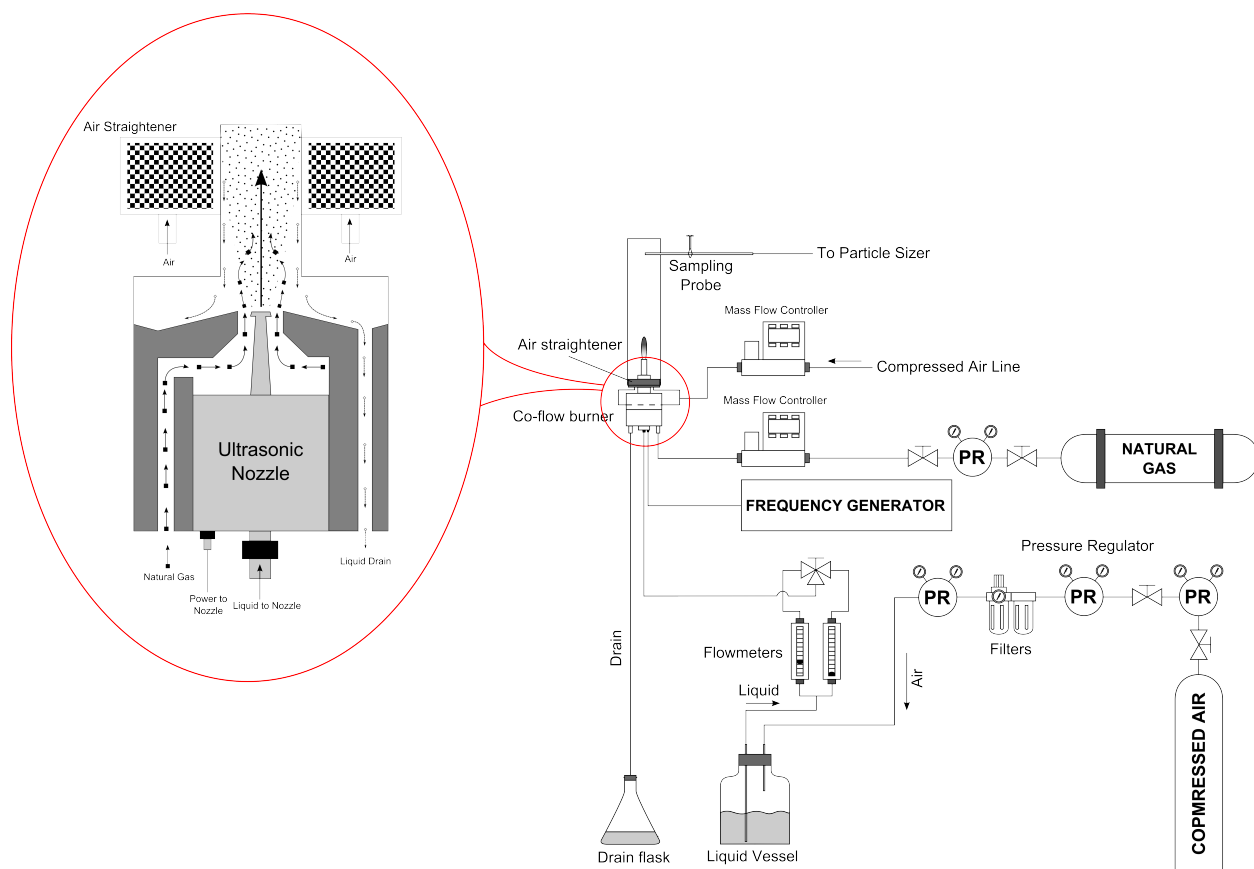

Figure 1. Schematic of the experiment setup for co-flow burner and liquid delivery system

3.   Results and Discussion

Experiments were performed to evaluate the effects of entrained droplets of distilled water, tap water, and salt water on particulate matter emissions of the co-flow laminar and sooting diffusion flames for each of the two flow conditions. For each droplet composition, the operating parameters remained unchanged so that the results could be compared. In addition, for each droplet composition, particle size distributions were obtained for both combusting and non-combusting cases to isolate changes in particulate emissions due to combustion.

3.1   Distilled Water Droplets in Flame Condition 1 (Lower Flow Rate)

Figure 2 shows the particle count distribution ($dN/d\log D_p$) with respect to mobility equivalent diameter when distilled water was injected into the fuel stream. The settings of the SMPS in this experiment gave a measurement range of 14.6 nm to 661.2 nm. This diagram plots particle size distributions in three cases as follows: (i) a non-reacting case with distilled water droplets atomized into the natural gas stream and transported upwards by the gas flow to the burner outlet, but without a flame present, (ii) the same conditions as (i) but with the flame present, and (iii) a base case with the flame present but without any water droplets injected into the flare gas. Both horizontal and vertical axes are shown in logarithmic scale to make the results visible when numbers change by orders of magnitude. Where the distribution line is not shown, it should be interpreted that no particles of that particular size were detected, since the logarithm of zero is not defined.

The particle counts in all three cases shown in Figure 2 were extremely small (the total number concentration in each case were 497 #/cm^3, 1.35×10^3 #/cm^3, and 639 #/cm^3; respectively). A clean combustion flame is expected when natural gas (mostly methane) is burned in this manner. Distilled water droplets contain no dissolved solid particles, therefore, low levels of particulate matter were expected.

3.2   Tap Water Droplets with Flame Condition 1 (Lower Flow Rate)

Figure 3 shows particle size distributions with and without a diffusion flame present when droplets of tap water were injected into the fuel stream. The flow rate of water was again fixed at 5.5 mL/min consistent with the results plotted in Figure 2. The tap water was extracted from the city of Edmonton water supply piping and had total dissolved mineral solids of 220 mg/L and total hardness of 169 mg CaCO$_3$/L [8]. Figure 3 shows that the particle counts at smaller sizes (<~70nm) were more than an order of magnitude higher when tap water droplets were sprayed into natural gas stream and combusted in a diffusion flame. The total number concentration in the each case was 2.65×10^3 #/cm^3 and 3.65×10^6 #/cm^3, respectively. Particle concentration was significantly higher at the lower range of particle sizes (14.6-30 nm), with maximum number occurring at a mobility diameter of 16.8 nm. The concentration also increased at the upper range of the particle diameter, but less significantly than for the small sized particles. The high number concentration of particulate matter in the combustion exhaust is attributable to the dissolved solid minerals in tap water.

3.3   Salt Water Droplets with Flame Condition 1 (Lower Flow Rate)

Since there was no reference in the literature about effects of salt water on gas flare emissions, an arbitrary concentration for the salt water was chosen in this study. By dissolving 100 g of sodium chloride in 900 g distilled water, a solution with NaCl mass fraction of 10% and density of 1110 kg/m^3 was obtained. Like all other experiments, the liquid delivery system was set to discharge 5.5 mL/min of salt water to the atomizer. Spraying salt water droplets into the diffusion flame affected its luminosity, giving the flame a bright yellow appearance, which is the characteristic colour of sodium in the flame. Particle size distribution measurements are plotted in Figure 4 for non-reacting and reacting cases. For the reacting case, additional measurements are plotted in which a thermodenuder was used in the sampling system. The thermodenuder heats up the exhaust sample to 200°C to evaporate any volatile material on the particles prior to their entering the SMPS for particle classification and counting. This allowed investigation of the importance of volatile materials in the particulate matter emissions.

Significant numbers of particles were present in the exhaust of the diffusion flame when combusting entrained salt-water droplets. The total number concentrations of particles were 3.48×10^3 #/cm^3 without the flame present, 6.21×10^7 #/cm^3 with the flame diffusion flame, and 4.26×10^7 #/cm^3 with the diffusion flame and thermodenuder. The maximum concentration of the particles occurs at a particle diameter of 91.4 nm. When the thermodenuder was inserted upstream of the SMPS, the log-normal distribution curve showed a slight shift towards larger particles, while the total number of particles was reduced by approximately 25% compared to the case without thermodenuder. This reduction in particle count can be attributed to diffusion losses or coagulation happening in the tubes before the SMPS as well as any volatile particles, which might be present in the exhaust. The thermodenuder results suggest that the particles that were formed were mostly solid since the number concentration or the size of the particles did not change significantly.

It is important to realize that the particles measured with the SMPS were not simply the dried NaCl/water droplets passing through the flame. Figure 5 shows the atomized droplet frequency distribution (according to specifications of the atomizer manufacturer) and the expected dried NaCl particle frequency distribution. The figure shows that the vast majority of the dried particles should be greater than 1 μm. Presumably the small dried NaCl particle concentration measured with the SMPS in Figure 4 (for the case of injected salt water without a diffusion flame present) is simply the left-hand tail of the distribution predicted in Figure 5. Therefore, the high particle concentration measured when the NaCl particles are burned can be attributed to the generation of new particles and not just the dried droplets passing through the flame. The mechanism for this new particle generation is not known. It seems likely that the high flame temperatures cause the NaCl droplets to evaporate (NaCl has a boiling point of 1413°C) and then nucleate to form a higher number of smaller particles. Future work will be conducted to explore these mechanisms.

3.4 Distilled Water Droplets with Flame Condition 2 (Higher Flow Rate Sooty Flame)

Figure 6 shows particle size distributions for the higher flow rate flame condition with and without entrained distilled water droplets. The flow rate of water was again fixed at 5.5 mL/min consistent with the results plotted in all other figures. The total number concentrations of particles were 8.56×10^6 #/cm^3 for the base case without entrained water droplets and 5.66×10^4 #/cm^3 with distilled water droplets injected into the fuel stream. Comparing the base-cases of the lower and higher flow conditions, the larger number of particles present in the exhaust is attributable to an increase in soot particles in the flame at the higher flow rate condition. The maximum number concentration of soot particles corresponded to a particle size of ~100 nm.

The presence of distilled water droplets in the higher flow rate (sooting) diffusion flame has a significant effect on suppression of particulate matter. Such an effect can be explained by the reduction of flame temperature in the soot generation zone, leading to a reduction in the number of soot particles being formed.

To investigate the presence of volatile compounds in the particulate matter, a thermodenuder was used upstream of SMPS. The results are shown in Figure 7 for the sooting diffusion flame with and without the thermodenuder, and in Figure 8 for the case where distilled water droplets are present in the sooting diffusion flame with and without thermodenuder. These results reveal that the particulate matter in the exhaust was non-volatile since there is no considerable shift in particle size distribution curves.

3.5 Salt Water Droplets in with Flame Condition 2 (Higher Flow Rate, Sooty Flame)

Particle size distribution plots are shown in Figure 9 for the sooting diffusion flame without salt water droplets (as the base case) and with salt water droplets. Consistent with the lower flow rate condition, a sodium chloride solution with 10% NaCl mass fraction was delivered to the ultrasonic atomizer at a flow rate of 5.5 mL/min. The total number concentration of particles in the flame exhaust for the base case without injected salt water droplets was 8.56×10^6 #/cm^3 compared with 3.51×10^7 #/cm^3 when salt water was injected into the fuel stream. The median particle size was ~100 nm for both cases.

The effect of salt water droplets in the sooting flame is interesting as combustion is very different when salt water droplets are present in the flame. The total number concentration of particulate matter emissions is increased by an order of 10 when salt water droplets are injected into the fuel stream. However, the additional particles do not seem to be soot and appear to have different characteristics than soot particles. Specifically, the particulate matter was white in colour and appeared to be a salt. It seems that salt water droplets may suppress soot formation but generate NaCl particles (presumably due to the nucleation of NaCl in the flame exhaust).

To investigate the importance of volatility in the particulate matter, the same thermodenuder was used upstream of SMPS. The results are shown in Figure 10 for the case where salt water droplets are present in the sooting diffusion flame with and without the thermodenuder. This figure shows that particulate matter emissions are mostly not volatile when salt water droplets are present in the fuel stream.

3.6 Gas-phase Emissions of with Flame Condition 2 (Higher Flow Rate, Sooty Flame)

Gas-phase analysis of the emissions of a sooting diffusion flame was done by means of portable gas analyzer Vetronix PXA-1100 manufactured by SPX Corporation. This unit was used to measure carbon monoxide, carbon dioxide, nitrogen oxides (NOx), and hydrocarbons in the exhaust. Three cases were studied as follows: sooting diffusion flame (as the base case), sooting diffusion flame with distilled water droplets at flow rate 5.5 mL/min, sooting diffusion flame with salt water (10% mass fraction) at flow rate 5.5 mL/min.

The results of gas-phase analysis is shown in Figure 11 as a bar chart with hydrocarbon (HC) and NOx concentrations in ppm and CO and CO_2 concentrations in volume percent (%). Uncertainty in measurements is indicated by full-line error bars on top of each data bar. These results reveal that when distilled water droplets are present in the flame, NOx and CO_2 level are decreased mainly due to local quenching effects of water in the flame where flame temperature is reduced. When salt water droplets are combusted in the sooting flame, hydrocarbon concentrations increase dramatically, mostly because of incomplete combustion of natural gas. NOx levels decrease compared to when distilled water droplets are present, implying that flame temperature is lower in the case of salt water droplets. Another indication of incomplete combustion with salt water droplets is high percentage of carbon monoxide in the exhaust (0.21% or 2100 ppmv) compared to the dry atmosphere (0.00001% or 0.1 ppmv).

3.7 Mass Measurement of Particulate Matter

A Centrifugal Particle Mass Analyzer (CPMA) designed and built at the University of Alberta was used to measure mass and density of the particles in the exhaust from a sooting diffusion flame. The CPMA uses opposing electrical and centrifugal forces to classify particles based on their mass, with the ability to vary the electrical field and rotation speed to select different particle masses. The CPMA was coupled with the DMA (same make and model as mentioned earlier in the experimental setup, connected upstream), and with the CPC (same make and model mentioned earlier, connected downstream). The DMA classified a narrow range of particle sizes (for instance, 100 nm), followed by the CPMA which measured the mass of the classified particles. Finally, the CPC was used to count the number of particles at the output of the CPMA. Such measurements were repeated over a wide range of particle sizes.

A preliminary density and mass measurement of soot particles from a sooting diffusion flame is shown in Figure 12. Particle mass increased as the particle size increased, however, soot density was reduced as particles grew larger in size due to the fractal shape of soot agglomerates with larger volumes. These effective density and mass measurements show a fractal dependency (i.e. they scale with a power law relationship) and are very typical for soot (like that from a Diesel engine for example). Particulate matter from sooting flame with distilled water droplets and with salt water droplets will be investigated by the mentioned procedure to determine their density and mass.

4. Concluding Remarks

The results presented in this report suggest that the effects of non-hydrocarbon liquids on gas flare emissions could be significant. However, the potential effects are complex and the exploratory results suggest that it is possible that salt water aerosols may actually suppress soot formation. The next steps in this study will include investigation of various fracturing liquid flow rates on exhaust emissions. Salt water with different salinity as well as hydrochloric acid solution will be tested in future studies. Further study into the nature of emitted particulate matter, (i.e. chemical composition by means of XPS and EDS analysis, morphology, and mass measurements) is also planned. Finally, further larger-scale testing in proposed at the new turbulent flare facility at the Carleton University using large (up to 4 m) turbulent flames which can better represent the flames typical of upstream flares found in the oil and gas industry.

References

[1] Intergovernment Panel on Climate Change, Climate Change 2007 - The Physical Science Basis, Contribution of Working Group I to the Fourth Assessment Report of the IPCC, Intergovernmental Panel on Climate Change, Geneva, 2007.

[2] U.S. Energy Information Administration, International Energy Statistics, Washington, DC, 2011. (Available at: http://www.eia.gov/cfapps/ipdbproject/IEDIndex3.cfm)

[3] M.R. Johnson, A.R. Coderre, An analysis of flaring and venting activity in the Alberta upstream oil and gas industry, *Journal of the Air and Waste Management Association* 61 (2) (2011) 190-200.

[4] J.D. Arthur, B. Bohm, M. Layne, Hydraulic Fracturing Considerations for Natural Gas Wells of the Marcellus Shale, The Ground Water Protection Council 2008 Annual Forum, Cincinnati, Ohio, Sept 21-24, 2008.

[5] A.M. Gomaa, M.A. Mahmoud, H.A. Nasr-El-Din, Effect of Shear Rate on the Propagation of Polymer-Based In-Situ-Gelled Acids Inside Carbonate Cores, *SPE Production & Operations* 26 (1) (2011) 41-54.

[6] United States Environmental Protection Agency, Evaluation of Impacts to Underground Sources of Drinking Water by Hydraulic Fracturing of Coalbed Methane Reservoirs, Washington, DC, 2004.

[7] United States House of Representatives: Committee on Energy and Commerce, Chemicals Used in Hydraulic Fracturing, Washington, DC, April 2011. (Available at: http://democrats.energycommerce.house.gov)

[8] EPCOR Utilities Inc., 2008 Edmonton Water Performance Report, EPCOR Utilities Incorporation, Edmonton, AB, 2008.